

New QCD Sum Rules for Nucleon Axial Vector Coupling Constants

Frank X. Lee

*TRIUMF, 4004 Wesbrook Mall Vancouver, BC, Canada V6T 2A3
and*

*Nuclear Physics Laboratory, Department of Physics,
University of Colorado, Boulder, CO 80309-0446, USA*

Derek B. Leinweber

Department of Physics, University of Washington, Seattle, WA 98195, USA

Xuemin Jin

*TRIUMF, 4004 Wesbrook Mall, Vancouver, BC, Canada V6T 2A3
and*

*Center for Theoretical Physics, Laboratory for Nuclear Science and Department of Physics,
Massachusetts Institute of Technology, Cambridge, MA 02139, USA*

Abstract

Two new sets of QCD sum rules for the nucleon axial coupling constants are derived using the external-field technique and generalized interpolating fields. An in-depth study of the predicative ability of these sum rules is carried out using a Monte-Carlo based uncertainty analysis. The results show that the standard implementation of the QCD sum rule method has only marginal predicative power for the nucleon axial coupling constants, as the relative errors are large. The errors range from approximately 50 to 100% compared to the nucleon mass obtained from the same method, which has only 10% to 25% error. The origin of the large errors is examined. Previous analyses of these coupling constants are based on sum rules that have poor OPE convergence and large continuum contributions. Preferred sum rules are identified and their predictions are obtained. We also investigate the new sum rules with an alternative treatment of the problematic transitions which are not exponentially suppressed in the standard treatment. The new treatment provides exponential suppression of their contributions relative to the ground state. Implications for other nucleon current matrix elements are

also discussed.

PACS numbers: 12.38.Lg, 11.40.Ha, 11.55.Hx, 14.20.Dh, 02.70.Lg

I. INTRODUCTION

Nucleon matrix elements of axial-vector currents at zero momentum transfer are characterized by the axial-vector coupling constants (or axial charges): isovector g_A , octet g_A^8 , isoscalar g_A^s , and flavor singlet g_A^0 . In terms of the quark spin content of the nucleon, one may express these coupling constants as:

$$\begin{aligned}
 g_A &= \Delta u - \Delta d, \\
 g_A^8 &= \Delta u + \Delta d - 2\Delta s, \\
 g_A^s &= \Delta u + \Delta d, \\
 g_A^0 &= \Delta u + \Delta d + \Delta s,
 \end{aligned}
 \tag{1}$$

where Δq is defined by $\langle ps | \bar{q} \gamma_\mu \gamma_5 q | ps \rangle \equiv \Delta q \bar{u}(p, s) \gamma_\mu \gamma_5 u(p, s)$ and $u(p, s)$ is a Dirac nucleon spinor. Knowledge of any three of the axial charges completely determines the quark spin content of the nucleon. Experimentally, $g_A \approx 1.26$ from neutron beta decay [1], $g_A^8 \approx 0.60$ [2], $g_A^s \approx 0.40$ from the EMC data together with strange-baryon decays [3], $g_A^0 \approx 0.22$ from SMC [4] and 0.27 from E143 [5]. These coupling constants reveal important information on the non-perturbative and non-valence structure of the nucleon. Obviously, understanding these quantities from QCD, the underlying theory of strong interactions, is an important theoretical issue. Within the framework of the QCD sum rule approach [6], these couplings have been previously studied in Refs. [7–12]. In the discussions to follow we will use g_A in a generic sense to mean all of these couplings.

Recently, a new Monte-Carlo based uncertainty analysis was introduced to quantitatively determine the predictive ability of QCD sum rules [15]. A comprehensive analysis of ground state ρ -meson and nucleon spectral properties was performed. Many of the findings contradicted the conventional wisdom of both practitioners and skeptics alike. In particular, careful consideration of operator product expansion (OPE) convergence and ground state dominance revealed that the nucleon sum rule traditionally favored in the QCD sum rule approach is invalid. Furthermore, it was found that the nucleon interpolating field advocated by Ioffe is not the optimal choice.

In this work, we will apply the Monte-Carlo method to the analysis of g_A . Our goal is to use this new analysis tool to determine the predicative ability of the QCD sum rule approach for g_A . This is the first application of such Monte-Carlo based analysis to a three-point function. Since previous studies of g_A are based on the Ioffe current and the invalid nucleon-mass sum rule, it is important to re-investigate g_A using alternate nucleon interpolating fields. To serve our purpose, two new sets of QCD sum rules are derived. One set is derived from a generalized correlator of spin-1/2 interpolating fields, and the other with a mixed correlator of spin-1/2 and spin-3/2 fields. We will examine all of the new sum rules and compare their performances.

The organization is as follows. Sec. II sets up the basic ingredients for calculating g_A using the external field method. In Sec. III, the QCD sum rules for the spin-1/2 correlator are presented and compared, wherever possible, with those obtained in previous works. In Sec. IV, the QCD sum rules for the mixed correlator are given, along with a discussion of the phenomenological representation. Results of the Monte-Carlo based sum rule analysis are presented in Sec. V. In Sec. VI we give an alternative treatment of the off-diagonal

transitions and compare with the standard treatment. The summary and conclusions are given in Sec. VII.

II. CALCULATION OF G_A USING THE EXTERNAL FIELD METHOD

The external field approach proceeds by adding an axial-vector coupling term to the QCD Lagrangian:

$$\Delta\mathcal{L} = - \sum_q g_q \bar{q} \hat{Z} \gamma_5 q, \quad (2)$$

and considering the two-point current correlation function in the presence of a constant axial vector external field:

$$\Pi(p) = i \int d^4x e^{ip \cdot x} \langle \Omega | T \{ \eta(x) \bar{\eta}(0) \} | \Omega \rangle_Z, \quad (3)$$

where $|\Omega\rangle$ denotes the QCD vacuum, Z is the axial vector external field and the hat notation denotes $\hat{Z} = Z^\alpha \gamma_\alpha$. The coupling g_q keeps track of the quark flavor in the external field. For example, if the external current is $J_\mu^5 = \bar{u} \gamma_\mu \gamma_5 u - \bar{d} \gamma_\mu \gamma_5 d$, then $g_u = -g_d = 1$, $g_s = 0$. In this way, we can obtain sum rules for all the couplings in the same calculation. To first order in the external field, $\Pi(p)$ is written as:

$$\Pi(p) = \Pi^{(0)}(p) + Z^\alpha \Pi_\alpha^{(1)}(p) + \dots \quad (4)$$

The axial vector coupling constant g_A is then extracted from the sum rules for the linear response $\Pi_\alpha^{(1)}(p)$. The external field couples directly to the quarks in the nucleon interpolating fields and polarizes the QCD vacuum. The latter can be described by the introduction of vacuum susceptibilities. The external field formalism is equivalent to the direct three-point function approach [14]; the resulting sum rules are identical.

A. Nucleon Interpolating Fields

The most general spin-1/2 nucleon interpolating current without derivatives can be written as

$$\eta_{1/2} = \eta_1 + \beta \eta_2, \quad (5)$$

where β is a real parameter and

$$\eta_1(x) = \epsilon^{abc} \left(u^{aT}(x) C \gamma_5 d^b(x) \right) u^c(x), \quad (6)$$

$$\eta_2(x) = \epsilon^{abc} \left(u^{aT}(x) C d^b(x) \right) \gamma_5 u^c(x). \quad (7)$$

The traditional current advocated by Ioffe in QCD sum rule calculations may be recovered by setting $\beta = -1$ and multiplying an overall factor of -2 :

$$\eta_N = 2(\eta_2 - \eta_1) = \epsilon^{abc} \left(u^{aT} C \gamma_\mu d^b \right) \gamma_5 \gamma^\mu u^c \quad (8)$$

However, we consider the generalized interpolator of (5) and select β to provide optimal sum rules [16].

In this work, we also consider the mixed correlator of the generalized case of Eq. (5):

$$\eta_{\mu,1/2} = \gamma_\mu \gamma_5 \eta_{1/2}, \quad (9)$$

with a spin-3/2 current which is also known to couple to the nucleon through its spin-1/2 component:

$$\eta_{\mu,3/2} = \epsilon^{abc} \left[(u^{aT} C \sigma_{\rho\lambda} d^b) \sigma^{\rho\lambda} \gamma_\mu u^c - (u^{aT} C \sigma_{\rho\lambda} u^b) \sigma^{\rho\lambda} \gamma_\mu d^c \right]. \quad (10)$$

The consideration of the mixed correlator is motivated by its success in nucleon mass sum rules [15,20]. There it is demonstrated that the sum rules from the mixed correlator have greater overlap with the ground state pole relative to the continuum contributions, have broader valid Borel regimes, and provide more stable estimates of spectral properties. It would be interesting to see if similar advantages can be gained here.

The matrix elements of the currents between the nucleon and the vacuum are defined as

$$\langle \Omega | \eta_{1/2} | N \rangle = \lambda_{1/2} u(p) \quad (11)$$

$$\langle \Omega | \eta_{\mu,3/2} | N \rangle = \lambda_{3/2} \left(\frac{4p_\mu}{M_N} + \gamma_\mu \right) \gamma_5 u(p). \quad (12)$$

where $u(p)$ denotes the Dirac spinor of the nucleon and λ describes the coupling strength of the currents to a nucleon state. We use the Dirac spinor normalization $\bar{u}(p)u(p) = 2M_N$.

B. Quark Propagator in the External Field

The calculation of the correlation function in the OPE requires the fully interacting quark propagator in coordinate space in the presence of the external axial-vector field. In the fixed-point gauge, the propagator up to order x^2 and Z is given by [7,8,10,15]

$$\begin{aligned} S_q^{ab}(x, 0; Z) &\equiv \langle \Omega | T \{ q^a(x) \bar{q}^b(0) \} | \Omega \rangle_Z \\ &= \frac{i}{2\pi^2} \frac{\hat{x}}{x^4} \delta^{ab} \\ &\quad - \frac{1}{12} \langle \bar{q}q \rangle \delta^{ab} \\ &\quad + \frac{i}{32\pi^2} (g_c G_{\alpha\beta}^n) \frac{\hat{x} \sigma^{\alpha\beta} + \sigma^{\alpha\beta} \hat{x}}{x^2} \frac{\lambda^{nab}}{2} \\ &\quad + \frac{1}{48} \frac{i}{32\pi^2} (g_c G_{\alpha\beta}^n) \frac{\hat{x} \sigma^{\alpha\beta} + \sigma^{\alpha\beta} \hat{x}}{x^2} \frac{\lambda^{nab}}{2} \\ &\quad - \frac{1}{192} \langle \bar{q} g_c \sigma \cdot G q \rangle \sigma^{\alpha\beta} \frac{\lambda^{ab}}{2} \end{aligned}$$

$$\begin{aligned}
& + \frac{1}{192} \langle \bar{q} g_c \sigma \cdot G q \rangle x^2 \delta^{ab} \\
& - \frac{g_q}{2\pi^2} \frac{(x \cdot Z) \hat{x} \gamma_5}{x^4} \delta^{ab} \\
& + \frac{i g_q}{36} \langle \bar{q} q \rangle (\hat{x} \hat{Z} - x \cdot Z) \gamma_5 \delta^{ab} \\
& + \frac{g_q}{12} \chi_v \langle \bar{q} q \rangle \hat{Z} \gamma_5 \delta^{ab} \\
& + \frac{g_q}{216} \kappa_v \langle \bar{q} q \rangle \left(\frac{5}{2} x^2 \hat{Z} - x \cdot Z \hat{x} \right) \gamma_5 \delta^{ab} \\
& - \frac{g_q}{96} \kappa_v \langle \bar{q} q \rangle (\hat{Z} \sigma^{\alpha\beta} + \sigma^{\alpha\beta} \hat{Z}) \gamma_5 \frac{\lambda^{nab}}{2} \\
& + \text{higher order terms.}
\end{aligned} \tag{13}$$

The external-field-induced vacuum susceptibilities χ_v and κ_v are defined by

$$\begin{aligned}
\langle \bar{q} \gamma_\mu \gamma_5 q \rangle_Z & \equiv \lim_{Q_\mu \rightarrow 0} (i Z_\nu) \int d^4 x e^{i Q \cdot x} \langle \Omega | T \left[\sum_q g_q \bar{q}(x) \gamma_\nu \gamma_5 q(x), \bar{q}(0) \gamma_\mu \gamma_5 q(0) \right] | \Omega \rangle \\
& \equiv g_q Z_\mu \chi_v \langle \bar{q} q \rangle,
\end{aligned} \tag{14}$$

and similarly,

$$\langle \bar{q} g_c \tilde{G}_{\mu\nu} \gamma^\nu q \rangle_Z \equiv g_q Z_\mu \kappa_v \langle \bar{q} q \rangle, \quad \tilde{G}_{\mu\nu} = \frac{1}{2} \epsilon_{\mu\nu\alpha\beta} G^{\alpha\beta}. \tag{15}$$

They describe the response of nonperturbative QCD vacuum to the external field.

III. QCD SUM RULES FOR THE SPIN-1/2 CORRELATOR

The calculation of the QCD side proceeds by contracting out the quark pairs in the correlation function:

$$\Pi(p) = i \int d^4 x e^{i p \cdot x} \langle \Omega | T \{ \eta_{1/2}(x) \bar{\eta}_{1/2}(0) \} | \Omega \rangle_Z, \tag{16}$$

where $\eta_{1/2}$ is given in Eq. (5), resulting in the following master formula before Fourier transformation:

$$\begin{aligned}
& \langle \Omega | T \{ \eta_{1/2}(x) \bar{\eta}_{1/2}(0) \} | \Omega \rangle_Z \\
& = -\epsilon^{abc} \epsilon^{a'b'c'} \{ \beta^2 \gamma_5 S_u^{aa'} \gamma_5 \text{Tr}(C S_d^{cc'T} C S_u^{bb'}) \\
& + S_u^{aa'} \text{Tr}(C S_d^{cc'T} C \gamma_5 S_u^{bb'} \gamma_5) \\
& + \beta \gamma_5 S_u^{aa'} \text{Tr}(C S_u^{cc'T} C S_d^{bb'} \gamma_5) \\
& + \beta S_u^{aa'} \gamma_5 \text{Tr}(C S_u^{cc'T} C \gamma_5 S_d^{bb'}) \\
& + S_u^{aa'} \gamma_5 C S_d^{cc'T} C \gamma_5 S_u^{bb'} \\
& + \beta \gamma_5 S_u^{aa'} \gamma_5 C S_d^{cc'T} C S_u^{bb'} \\
& + \beta S_u^{aa'} C S_d^{cc'T} C \gamma_5 S_u^{bb'} \gamma_5 \\
& + \beta^2 \gamma_5 S_u^{aa'} C S_d^{cc'T} C S_u^{bb'} \gamma_5 \},
\end{aligned} \tag{17}$$

where

$$S_q^{ab}(x, 0; Z) \equiv \langle \Omega | T \{ q^a(x) \bar{q}^b(0) \} | \Omega \rangle_Z, \quad (18)$$

is the quark propagator given in Eq. (13). As discussed above, we are only concerned with the linear response of the correlator to the external field. When substituting the quark propagator into Eq. (17), we keep terms only to first order in the external field. The results after Fourier transform have three distinct Dirac structures and can be organized by the invariant functions:

$$Z \cdot \Pi^{(1)}(p^2) = \Pi_1(p^2) \hat{Z} \gamma_5 + \Pi_2(p^2) Z \cdot p \hat{p} \gamma_5 + \Pi_3(p^2) i Z_\mu \sigma^{\mu\nu} p_\nu \gamma_5. \quad (19)$$

Three sum rules can be derived from the invariant functions. To save space, the invariant functions are not written out explicitly. But they can be easily inferred from the sum rules below. The sum rules after Borel transform are as follows. At structure $\hat{Z} \gamma_5$:

$$\begin{aligned} & \frac{1}{64} [(\beta^2 + 1)(6g_u + g_d) + 2\beta(6g_u + 5g_d)] E_2 L^{-4/9} M^6 \\ & - \frac{1}{24} [(\beta^2 + 1)(9g_u - g_d) + 8\beta g_u] \chi_v a E_1 L^{-4/9} M^4 \\ & + \frac{1}{256} [(\beta^2 + 1)(6g_u - g_d) + 2\beta(2g_u - g_d)] b E_0 L^{-4/9} M^2 \\ & + \frac{1}{48} [(\beta^2 + 1)(21g_u + g_d) + 2\beta(5g_u - 3g_d)] \kappa_v a E_0 L^{-68/81} M^2 \\ & - \frac{1}{72} [(\beta^2(18g_u + 5g_d) - 2\beta(2g_u + 3g_d) - 14g_u + g_d)] a^2 L^{4/9} \\ & - \frac{1}{288} [5(\beta^2 + 1)g_u + \beta(3g_u - g_d)] \chi_v a b L^{-4/9} \\ & = \tilde{\lambda}_{1/2}^2 \left[g_A \left(1 - \frac{2M_N^2}{M^2} \right) + A \right] e^{-M_N^2/M^2}, \end{aligned} \quad (20)$$

at structure $Z \cdot p \hat{p} \gamma_5$:

$$\begin{aligned} & \frac{1}{64} [(\beta^2 + 1)(6g_u + g_d) + 2\beta(6g_u + 5g_d)] E_1 L^{-4/9} M^4 \\ & - \frac{1}{48} [(\beta^2 + 1)g_d + 2\beta(2g_u + 3g_d)] \chi_v a E_0 L^{-4/9} M^2 \\ & + \frac{1}{256} [(\beta^2 + 1)(6g_u - g_d) + 2\beta(2g_u - g_d)] b L^{-4/9} \\ & - \frac{1}{144} [(\beta^2 + 1)(9g_u + 5g_d) + 10\beta(g_u + g_d)] \kappa_v a L^{-68/81} \\ & - \frac{1}{72} [\beta^2(18g_u + g_d) + 2\beta(2g_u - 3g_d) + (-22g_u + 5g_d)] a^2 L^{4/9} \frac{1}{M^2} \\ & + \frac{1}{1152} [(\beta^2 + 1)(2g_u + 3g_d) + 2\beta g_d] \chi_v a b L^{-4/9} \frac{1}{M^2} \\ & = \tilde{\lambda}_{1/2}^2 \left[\frac{g_A}{M^2} + A \right] e^{-M_N^2/M^2}, \end{aligned} \quad (21)$$

and at structure $iZ_\mu\sigma^{\mu\nu}p_\nu\gamma_5$:

$$\begin{aligned}
& -\frac{1}{48} [\beta^2(6g_u + g_d) - 2\beta g_d - (6g_u - g_d)] a E_0 L^{2/9} M^2 \\
& +\frac{1}{24} [(\beta^2 g_d - 2\beta g_u + 2g_u - g_d) \chi_v a^2 \\
& -\frac{1}{432} [\beta^2(6g_u + 7g_d) - 26\beta g_u + 20g_u - 7g_d] \kappa_v a^2 L^{-32/81} \frac{1}{M^2} \\
& -\frac{1}{576} [\beta^2(2g_u + 7g_d) - 6\beta g_u + 4g_u - 7g_d] \chi_v m_0^2 a^2 L^{-14/27} \frac{1}{M^2} \\
& = \tilde{\lambda}_{1/2}^2 \left[\frac{g_A M_N}{M^2} + A \right] e^{-M_N^2/M^2}. \tag{22}
\end{aligned}$$

Here and in the following, $a = -(2\pi)^2 \langle \bar{q}q \rangle$, $b = \langle g_c^2 G^2 \rangle$, $\langle \bar{q}g_c\sigma \cdot Gq \rangle = -m_0^2 \langle \bar{q}q \rangle$, $\tilde{\lambda}_{1/2} = (2\pi)^2 \lambda_{1/2}$. As usual, the anomalous dimension corrections of the various operators are taken into account via the factor $L = [\alpha_s(\mu^2)/\alpha_s(M^2)] = [\ln(M^2/\Lambda_{QCD}^2)/\ln(\mu^2/\Lambda_{QCD}^2)]$, where $\mu = 500$ MeV is the renormalization scale and Λ_{QCD} is the QCD scale parameter which will be given later. The factors $E_n(x) = 1 - e^{-x} \sum_n x^n/n!$ with $x = w^2/M^2$ account for the excited state contributions, where w is an effective continuum threshold. The parameter A is introduced to account for all contributions from transitions between the nucleon ground state and the excited states; such a treatment is an approximation and may lead to errors in the extracted ground state property (see Sec. IV A below). The continuum threshold and transition strength are *a priori* unknown. So one should bear in mind that they are in principle different for different sum rules. We will treat them as parameters and study their roles in the analysis.

The sum rules for g_A can be obtained by setting $g_u = -g_d = 1$ in Eq. (20) to Eq. (22), while the sum rules for g_A^s , g_A^8 , g_A^0 can be obtained by setting $g_u = g_d = 1$. Note that the three axial couplings g_A^s , g_A^8 , g_A^0 share the same set of sum rules. The difference lies in the susceptibilities χ_v and κ_v .

At this point, comparisons can be made with the sum rules obtained in previous works using the Ioffe current by setting $\beta = -1$ and $\lambda_{1/2}^2 = \lambda_N^2/4$ in Eq. (20) to Eq. (22). For the most part, we find that our sum rules for g_A agree with those of Refs. [7–10], with only a few exceptions. There are differences in the anomalous dimension corrections to the terms involving the mixed condensate. We use $-2/27$ for the anomalous dimension of the mixed condensate, while previous works simply used 0. The dimension 7 operator $\chi_v ab$, which is considered in this work and in Ref. [10], differs at structures $\hat{Z}\gamma_5$ and $Z \cdot p\hat{p}\gamma_5$. Also, the coefficient in front of the dimension 7 operator $\kappa_v a^2$ at structure $iZ_\mu\sigma^{\mu\nu}p_\nu\gamma_5$ disagrees with that of Ref. [8]. For the other axial couplings, comparisons can only be made at structure $Z \cdot p\hat{p}\gamma_5$. We find that our sum rules agree with those of Refs. [9,10], but again report corrections for the $\chi_v ab$ term.

IV. QCD SUM RULES FOR THE MIXED CORRELATOR

The correlation function we consider is

$$\Pi_{\mu\nu}(p) = i \int d^4x e^{ip \cdot x} \langle \Omega | T \{ \eta_{\mu,1/2}(x) \bar{\eta}_{\nu,3/2}(0) \} | \Omega \rangle_Z, \quad (23)$$

where $\eta_{\mu,1/2}$ is given in Eq. (9) and $\eta_{\mu,3/2}$ is given in Eq. (10). In the following, we first discuss the phenomenological representation of the correlation function, then calculate the QCD side using the OPE.

A. Phenomenological Ansatz for the Mixed Correlator

The linear response of the correlation function in the external field can be written as:

$$Z \cdot \Pi_{\mu\nu}^{(1)}(p) = (-iZ^\alpha) i \int d^4x e^{ip \cdot x} \langle \Omega | T \{ \eta_{\mu,1/2}(x) \int d^4y J_\alpha^5(y) \bar{\eta}_{\nu,3/2}(0) \} | \Omega \rangle. \quad (24)$$

After inserting two complete sets of intermediate physical states and carrying out the integrations, one has:

$$\begin{aligned} \Pi_{\mu\nu}^{(1)}(p, Z) &= Z^\alpha \sum_{BB'} \frac{-1}{(p^2 - M_B^2)(p^2 - M_{B'}^2)} \\ &\quad \sum_{ss'} \langle \Omega | \eta_{\mu,1/2} | Bps \rangle \langle Bps | J_\alpha^5 | B'ps' \rangle \langle B'ps' | \bar{\eta}_{\nu,3/2} | \Omega \rangle. \end{aligned} \quad (25)$$

The axial current coupling constant enters via the nucleon matrix element:

$$\langle Nps | J_\alpha^5 | Nps \rangle \equiv g_A \bar{u}(p, s) \gamma_\alpha \gamma_5 u(p, s). \quad (26)$$

To determine the Dirac structure, let us look at the ground state contribution to Eq. (25) after the spin sums:

$$\begin{aligned} Z \cdot \Pi_{\mu\nu}^{(1)} &= \frac{-\lambda_{1/2} \lambda_{3/2} g_A}{(p^2 - M_N^2)^2} \gamma_\mu \gamma_5 (\hat{p} + M_N) \hat{Z} \gamma_5 (\hat{p} + M_N) \gamma_\nu \left(\frac{4p_\nu}{M_N} + \gamma_\nu \right) \\ &= \frac{-\lambda_{1/2} \lambda_{3/2} g_A}{(p^2 - M_N^2)^2} \left[(p^2 + M_N^2) \gamma_\mu \gamma_5 \hat{Z} \gamma_\nu + \frac{4(p^2 + M_N^2)}{M_N} \gamma_\mu \gamma_5 \hat{Z} p_\nu - 2 \gamma_\mu \gamma_5 (Z \cdot p) \hat{p} \gamma_\nu \right. \\ &\quad \left. - \frac{8}{M_N} \gamma_\mu \gamma_5 (Z \cdot p) \hat{p} p_\nu - 2M_N \gamma_\mu \gamma_5 (\hat{Z} \hat{p} - Z \cdot p) \gamma_\nu - 8 \gamma_\mu \gamma_5 (\hat{Z} \hat{p} - Z \cdot p) p_\nu \right]. \end{aligned} \quad (27)$$

We see that there are eight distinct structures from which eight sum rules can be derived.

The pole structure of the correlation function from Eq. (25) can be written as

$$\frac{\lambda_{1/2} \lambda_{3/2} g_A}{(p^2 - M_N^2)^2} + \sum_{N^*} \frac{C_{N \leftrightarrow N^*}}{(p^2 - M_N^2)(p^2 - M_{N^*}^2)} + \sum_{N^*} \frac{D_{N^* \rightarrow N^*}}{(p^2 - M_{N^*}^2)^2}, \quad (28)$$

where $C_{N \leftrightarrow N^*}$ and $D_{N \leftrightarrow N^*}$ are constants. The first term is the ground state double pole, the second term represents the non-diagonal transitions between the nucleon and the excited states caused by the external field, and the third term represents the excited state contributions. Upon Borel transform, one has

$$\begin{aligned}
& \frac{\lambda_{1/2}\lambda_{3/2} g_A}{M^2} e^{-M_N^2/M^2} + e^{-M_N^2/M^2} \left[\sum_{N^*} \frac{C_{N \rightarrow N^*}}{M_N^2 - M_{N^*}^2} \left(1 - e^{-(M_{N^*}^2 - M_N^2)/M^2} \right) \right] \\
& + \sum_{N^*} \frac{D_{N^* \rightarrow N^*}}{M_{N^*}^2} e^{-M_{N^*}^2/M^2}.
\end{aligned} \tag{29}$$

We see that the transitions (second term) give rise to a contribution that is not exponentially suppressed relative to the ground state (first term). The strength of such transitions at each structure is *a priori* unknown and is an additional source of contamination in the determination of g_A not found in mass sum rules. The usual treatment of the transitions is to approximate the quantity in the square brackets by a constant phenomenological parameter, which is to be extracted from the sum rule along with the ground state property of interest. Such an approximation has been adopted in the sum rules (20) to (22). Here we want to stress that the transition term is in fact a complicated function of the Borel mass and the usual approximation alters the curvature of the phenomenological side and hence introduces errors in the extracted ground state property. Later in this work, we will present an alternative method of treating such transitions, which provides exponential suppression of the transitions relative to the ground state contribution. The pure excited state contributions (the last term) are exponentially suppressed relative to the ground state and can be modeled in the usual way by introducing a continuum model and threshold parameter.

B. Calculation of the QCD side

The master formula is given by

$$\begin{aligned}
& \langle \Omega | T \{ \eta_{\mu,1/2}(x) \bar{\eta}_{\nu,3/2}(0) \} | \Omega \rangle_Z \\
& = \epsilon^{abc} \epsilon^{a'b'c'} \{ \beta \gamma_\mu S_u^{aa'} \gamma_\nu \sigma_{\rho\lambda} \text{Tr}(S_d^{bb'} \sigma^{\rho\lambda} C S_u^{cc'T} C) \\
& + \gamma_\mu \gamma_5 S_u^{aa'} \gamma_\nu \sigma_{\rho\lambda} \text{Tr}(\gamma_5 S_d^{bb'} \sigma^{\rho\lambda} C S_u^{cc'T} C) \\
& - 2 \gamma_\mu \gamma_5 S_u^{aa'} \sigma_{\rho\lambda} C S_u^{cc'T} C \gamma_5 S_d^{bb'} \gamma_\nu \sigma^{\rho\lambda} \\
& - \gamma_\mu \gamma_5 S_u^{aa'} \sigma_{\rho\lambda} C S_d^{cc'T} C \gamma_5 S_u^{bb'} \gamma_\nu \sigma^{\rho\lambda} \\
& - 2 \beta \gamma_\mu S_u^{aa'} \sigma_{\rho\lambda} C S_u^{cc'T} C S_d^{bb'} \gamma_\nu \sigma^{\rho\lambda} \\
& - \beta \gamma_\mu S_u^{aa'} \sigma_{\rho\lambda} C S_d^{cc'T} C S_u^{bb'} \gamma_\nu \sigma^{\rho\lambda} \}.
\end{aligned} \tag{30}$$

The calculation proceeds in the same way as in the spin-1/2 case by substituting the quark propagator into Eq. (30), keeping terms to first order in the external field. The results after Fourier transform have eight distinct Dirac structures and can be organized as

$$\begin{aligned}
Z \cdot \Pi_{\mu\nu}^{(1)}(p^2) & = \Pi_1(p^2) \gamma_\mu \gamma_5 \hat{Z} \gamma_\nu + \Pi_2(p^2) \gamma_\mu \gamma_5 \hat{Z} p_\nu + \Pi_3(p^2) \gamma_\mu \gamma_5 (Z \cdot p) \gamma_\nu \\
& + \Pi_4(p^2) \gamma_\mu \gamma_5 (Z \cdot p) p_\nu + \Pi_5(p^2) \gamma_\mu \gamma_5 \hat{Z} \hat{p} \gamma_\nu + \Pi_6(p^2) \gamma_\mu \gamma_5 \hat{Z} \hat{p} p_\nu \\
& + \Pi_7(p^2) \gamma_\mu \gamma_5 (Z \cdot p) \hat{p} \gamma_\nu + \Pi_8(p^2) \gamma_\mu \gamma_5 (Z \cdot p) \hat{p} p_\nu.
\end{aligned} \tag{31}$$

After Borel transform, eight sum rules are obtained. They are as follows. At structure $\gamma_\mu \gamma_5 \hat{Z} \gamma_\nu$:

$$\begin{aligned}
& -\frac{(1-\beta)(g_u-g_d)}{4} \chi_v a E_1 L^{-4/27} M^4 \\
& -\frac{(1-\beta)(g_u-g_d)}{18} \kappa_v a E_0 L^{-44/81} M^2 - \frac{(1-\beta)(g_u-g_d)}{96} b E_0 L^{-4/27} M^2 \\
& + \frac{\beta(7g_u+5g_d)+10g_u}{9} a^2 L^{20/27} + \frac{(1-\beta)(g_u-g_d)}{96} \chi_v a b L^{-4/27} \\
& = \tilde{\lambda}_{1/2} \tilde{\lambda}_{3/2} \left[g_A \left(1 - \frac{2M_N^2}{M^2}\right) + A \right] e^{-M_N^2/M^2}, \tag{32}
\end{aligned}$$

at structure $\gamma_\mu \gamma_5 \hat{Z} p_\nu$:

$$\begin{aligned}
& \frac{3\beta(g_u+g_d)+11g_u-2g_d}{18} a E_0 L^{8/27} M^2 \\
& + \frac{3\beta(5g_u+7g_d)+19g_u-7g_d}{96} m_0^2 a L^{-2/9} - \frac{\beta(g_u-g_d)+7g_u-g_d}{6} \chi_v a^2 L^{8/27} \\
& + \frac{\beta(g_u-7g_d)+19g_u-7g_d}{144} \chi_v m_0^2 a^2 L^{-2/9} \frac{1}{M^2} \\
& + \frac{\beta(g_u+11g_d)-3(8g_u+g_d)}{54} \kappa_v a^2 L^{-8/81} \frac{1}{M^2} \\
& = \tilde{\lambda}_{1/2} \tilde{\lambda}_{3/2} \left[\frac{g_A}{M_N} \left(1 - \frac{2M_N^2}{M^2}\right) + A \right] e^{-M_N^2/M^2}, \tag{33}
\end{aligned}$$

at structure $\gamma_\mu \gamma_5 Z \cdot p \gamma_\nu$:

$$\begin{aligned}
& \frac{12\beta(g_u+g_d)+8g_u+g_d}{18} a E_0 L^{8/27} M^2 - \frac{\beta(g_u+2g_d)}{3} \chi_v a^2 L^{-8/27} \\
& + \frac{7\beta(g_u+2g_d)}{72} \chi_v m_0^2 a^2 L^{-2/9} \frac{1}{M^2} + \frac{\beta(59g_u+55g_d)+9(5g_u-g_d)}{108} \kappa_v a^2 L^{-8/81} \frac{1}{M^2} \\
& = \tilde{\lambda}_{1/2} \tilde{\lambda}_{3/2} \left[\frac{g_A M_N}{M^2} + A \right] e^{-M_N^2/M^2}, \tag{34}
\end{aligned}$$

at structure $\gamma_\mu \gamma_5 Z \cdot pp_\nu$:

$$\begin{aligned}
& \frac{(1-\beta)(g_u-g_d)}{12} \chi_v a E_0 L^{-4/27} M^2 \\
& - \frac{5(1-\beta)(g_u-g_d)}{36} \kappa_v a L^{-44/81} - \frac{(1-\beta)(g_u-g_d)}{96} b L^{-4/27} \\
& + \frac{4\beta(2g_u+g_d)+5g_u+2g_d}{18} a^2 L^{20/27} \frac{1}{M^2} + \frac{(1-\beta)(g_u-g_d)}{288} \chi_v a b L^{-4/27} \frac{1}{M^2} \\
& = \tilde{\lambda}_{1/2} \tilde{\lambda}_{3/2} \left[\frac{g_A}{M^2} + A \right] e^{-M_N^2/M^2}, \tag{35}
\end{aligned}$$

at structure $\gamma_\mu \gamma_5 \hat{Z} \hat{p} \gamma_\nu$:

$$\frac{3\beta(g_u+g_d)-g_u+g_d}{12} a E_0 L^{8/27} M^2 - \frac{\beta(g_u+5g_d)-7g_u+g_d}{12} \chi_v a^2 L^{8/27}$$

$$\begin{aligned}
& + \frac{\beta(13g_u + 35g_d) - 19g_u + 7g_d}{288} \chi_v m_0^2 a^2 L^{8/27} \frac{1}{M^2} \\
& + \frac{\beta(31g_u + 47g_d) - 73g_u - 5g_d}{216} \kappa_v a^2 L^{-8/81} \frac{1}{M^2} \\
& = \tilde{\lambda}_{1/2} \tilde{\lambda}_{3/2} \left[\frac{g_A M_N}{M^2} + A \right] e^{-M_N^2/M^2}, \tag{36}
\end{aligned}$$

at structure $\gamma_\mu \gamma_5 \hat{Z} \hat{p} p_\nu$:

$$\begin{aligned}
& \frac{(1-\beta)(g_u - g_d)}{24} \chi_v a E_0 L^{-4/27} M^2 - \frac{7(1-\beta)(g_u - g_d)}{144} \kappa_v a L^{-44/81} \\
& + \frac{\beta(g_u - g_d) + 8g_u - g_d}{18} a^2 L^{20/27} \frac{1}{M^2} + \frac{(1-\beta)(g_u - g_d)}{576} \chi_v a b L^{-4/27} \frac{1}{M^2} \\
& = \tilde{\lambda}_{1/2} \tilde{\lambda}_{3/2} \left[\frac{g_A}{M^2} + A \right] e^{-M_N^2/M^2}, \tag{37}
\end{aligned}$$

at structure $\gamma_\mu \gamma_5 Z \cdot p \hat{p} \gamma_\nu$:

$$\begin{aligned}
& \frac{(1-\beta)(g_u - g_d)}{12} \chi_v a E_0 L^{-4/27} M^2 \\
& - \frac{5(1-\beta)(g_u - g_d)}{36} \kappa_v a L^{-44/81} - \frac{(1-\beta)(g_u - g_d)}{96} b L^{-4/27} \\
& + \frac{2(1+\beta) + 3g_u + g_d}{9} a^2 L^{20/27} \frac{1}{M^2} + \frac{(1-\beta)(g_u - g_d)}{288} \chi_v a b L^{-4/27} \frac{1}{M^2} \\
& = \tilde{\lambda}_{1/2} \tilde{\lambda}_{3/2} \left[\frac{g_A}{M^2} + A \right] e^{-M_N^2/M^2}, \tag{38}
\end{aligned}$$

and at structure $\gamma_\mu \gamma_5 Z \cdot p \hat{p} p_\nu$:

$$\begin{aligned}
& \frac{3\beta(g_u + g_d) + 11g_u - 2g_d}{18} a L^{8/27} - \frac{3\beta(5g_u + 7g_d) + 19g_u - 7g_d}{96} m_0^2 a L^{-2/9} \frac{1}{M^2} \\
& - \frac{3\beta(g_u + g_d) + 7g_u - g_d}{27} \kappa_v a^2 L^{-8/81} \frac{1}{M^4} \\
& = \tilde{\lambda}_{1/2} \tilde{\lambda}_{3/2} \left[\frac{g_A}{M_N M^2} + A \right] e^{-M_N^2/M^2}. \tag{39}
\end{aligned}$$

V. MONTE CARLO SUM RULE ANALYSIS

The reader is referred to Ref. [15] for a complete description of the method. The basic steps are as follows. One first generates many sets of randomly-selected, Gaussianly-distributed QCD parameter sets, from which an uncertainty distribution in the OPE can be constructed. Then a χ^2 minimization is applied to the sum rule by adjusting the phenomenological fit parameters. This is done for each QCD parameter set, resulting in distributions for phenomenological fit parameters, from which errors are derived. Usually, 100 such configurations are sufficient for getting stable results. We generally select 1000 which help

resolve more subtle correlations among the QCD parameters and the phenomenological fit parameters.

The Borel window over which the two sides of a sum rule are matched is determined by the following two criteria: a) *OPE convergence* — the highest-dimension-operators contribute no more than 10% to the QCD side when $\beta = 0$, b) *ground-state dominance* — all excited state contributions (including transitions) are no more than 50% of the phenomenological side. Those sum rules which do not have a valid Borel window are considered unreliable and therefore discarded. The emphasis here is on exploring the QCD parameter space via Monte Carlo. The 10%-50% criteria are a reasonable choice that provide a basis for quantitative analysis. Reasonable alternatives to the 10%-50% criteria are automatically explored in the Monte-Carlo analysis, as the condensate values and the continuum threshold change in each sample.

A. QCD Input Parameters

The QCD input parameters and their uncertainty assignments are given as follows. The quark condensate is taken as $a = 0.52 \pm 0.05 \text{ GeV}^3$. A number of recent studies [15] prefer much larger values for the gluon condensate than early estimates of $0.47 \pm 0.2 \text{ GeV}^4$ from charmonium sum rules. Hence we adopt $b = 1.2 \pm 0.6 \text{ GeV}^4$ with 50% uncertainty. The mixed condensate parameter is placed at $m_0^2 = 0.72 \pm 0.08 \text{ GeV}^2$. Note that the value of the mixed condensate itself is obtained by multiplying the randomly-selected m_0^2 with the central value of the quark condensate. Factorization violation of the four quark operators is parameterized as $\kappa \langle \bar{q}q \rangle^2$, where we consider $\kappa = 2 \pm 1$ and $1 \leq \kappa \leq 4$. The QCD scale parameter Λ_{QCD} is restricted to the values conventionally adopted in the QCD sum rule approach: $\Lambda_{QCD} = 0.15 \pm 0.04 \text{ GeV}$, and $0.10 \text{ GeV} \leq \Lambda_{QCD} \leq 0.20 \text{ GeV}$. Variation of Λ_{QCD} has little effects on the results.

The external-field-induced vacuum susceptibilities for the isovector g_A have been estimated previously [7,8,13]. We consider $\chi_v a = 0.70 \pm 0.05 \text{ GeV}^2$ and $\kappa_v a = 0.14 \pm 0.14 \text{ GeV}^4$. $\chi_v a$ is related to PCAC which is well known. κ_v is related to the matrix element $\langle 0 | \bar{q} g_c \tilde{G}_{\mu\nu} \gamma^\nu q | \pi \rangle_Z$ which is not well determined. Note that the combinations $\chi_v a$ and $\kappa_v a$ as a whole are selected by Monte Carlo. For the flavor singlet g_A^0 , they have been estimated in Ref. [12]. Here we adopt them with 50% and 100% uncertainties, respectively: $\chi_v a = 0.14 \pm 0.07 \text{ GeV}^2$, $\kappa_v a = 0.01 \pm 0.01 \text{ GeV}^4$.

For the octet g_A^8 and isoscalar g_A^s , the susceptibilities are estimated from the following consideration. Nucleon matrix elements $\langle \bar{q} \gamma_\mu \gamma_5 q \rangle$ have a connected (valence) contribution, as well as a quark loop contribution connected only by gluons. Lattice studies [17] found that the loop contributions are almost independent of the quark flavors u, d and s. In the limit of equal loop contributions for u, d and s quarks, both g_A and g_A^8 have the loop contributions cancelled out, leaving only the valence contributions, as shown in Eq.(1). Hence, we assume the susceptibilities are the same for these two couplings. On the other hand, g_A^0 has valence plus three flavors of loop contributions, and g_A^s has valence plus two flavors of loop contributions. From these arguments one can express the susceptibilities for g_A^s in terms of those for g_A and g_A^0 . They are estimated as $\chi_v = 0.33 \pm 0.16$ and $\kappa_v = 0.05 \pm 0.05$, where we have assigned 50% and 100% uncertainties, respectively.

These uncertainties are assigned conservatively and in accord with the state-of-the-art in the literature. While some may argue that some values are better known, others may find that the errors are underestimated. In any event, one will learn how the uncertainties in the QCD parameters are mapped into uncertainties in the phenomenological fit parameters. Fig. 1 shows distributions for these QCD parameters drawn from a sample of 1000 sets.

B. Search Procedure

In principle, one can extract g_A from any of the sum rules presented earlier. In practice, however, some sum rules work better than others. This is because one works with a truncated OPE series, which may have different convergence properties at different structures. By selecting appropriate mixing of the components of the generalized interpolating fields, one can minimize the overlap with excited states, and broaden the regime in Borel space where both sides of the sum rule are under reasonable control. In the following, we use the optimal $\beta = -1.2$ for the spin-1/2 sum rules and $\beta = 0$ for the mixed sum rules, as determined in Ref. [15].

The analysis of g_A sum rules requires the corresponding nucleon mass sum rules for normalization. They are taken from Ref. [15] for the spin-1/2 correlator at structure 1:

$$\begin{aligned} & \frac{7 - 2\beta - 5\beta^2}{16} a E_1 M^4 - \frac{3(1 - \beta^2)}{16} m_0^2 a E_0 L^{-14/27} M^2 \\ & + \frac{19 + 10\beta - 29\beta^2}{2^7 3^2} a b = \tilde{\lambda}_{1/2}^2 M_N e^{-M_N^2/M^2}. \end{aligned} \quad (40)$$

Note that we use the nucleon mass sum rule at the chirally-even structure 1, rather than the traditionally favored one at the the chirally-odd structure \hat{p} , since the latter was found to be invalid [15]. The optimal fit parameters obtained from consideration of 1000 QCD parameter sets are

$$M_N = 1.17 \pm 0.26 \text{ GeV}, \quad \tilde{\lambda}_{1/2}^2 = 0.20 \pm 0.12 \text{ GeV}^6, \quad w_N = 1.53 \pm 0.41 \text{ GeV}, \quad , \quad (41)$$

For the mixed correlator, we use the nucleon mass sum rules at structure $\gamma_\mu \gamma_\nu$

$$\frac{1}{2} a L^{8/27} E_1 M^4 + \frac{1 + 3\beta}{96} a b L^{8/27} = \tilde{\lambda}_{1/2} \tilde{\lambda}_{3/2} M_N e^{-M_N^2/M^2}, \quad (42)$$

and at structure $\gamma_\mu \hat{p} p_\nu$

$$\frac{1}{2} a L^{8/27} E_0 M^2 - \frac{3 - \beta}{16} m_0^2 a L^{-2/9} - \frac{1 + 3\beta}{96} \frac{a b}{M^2} L^{8/27} = \tilde{\lambda}_{1/2} \tilde{\lambda}_{3/2} M_N e^{-M_N^2/M^2}. \quad (43)$$

A combined analysis of the two sum rules from consideration of 1000 QCD parameter sets gives

$$M_N = 0.96 \pm 0.08 \text{ GeV}, \quad \tilde{\lambda}_{1/2} \tilde{\lambda}_{3/2} = 0.41 \pm 0.14 \text{ GeV}^6, \quad w_N = 1.3 \pm 0.2 \text{ GeV}, \quad . \quad (44)$$

Note that the parameters determined from the mixed correlator have much smaller uncertainty than from the spin-1/2 correlator.

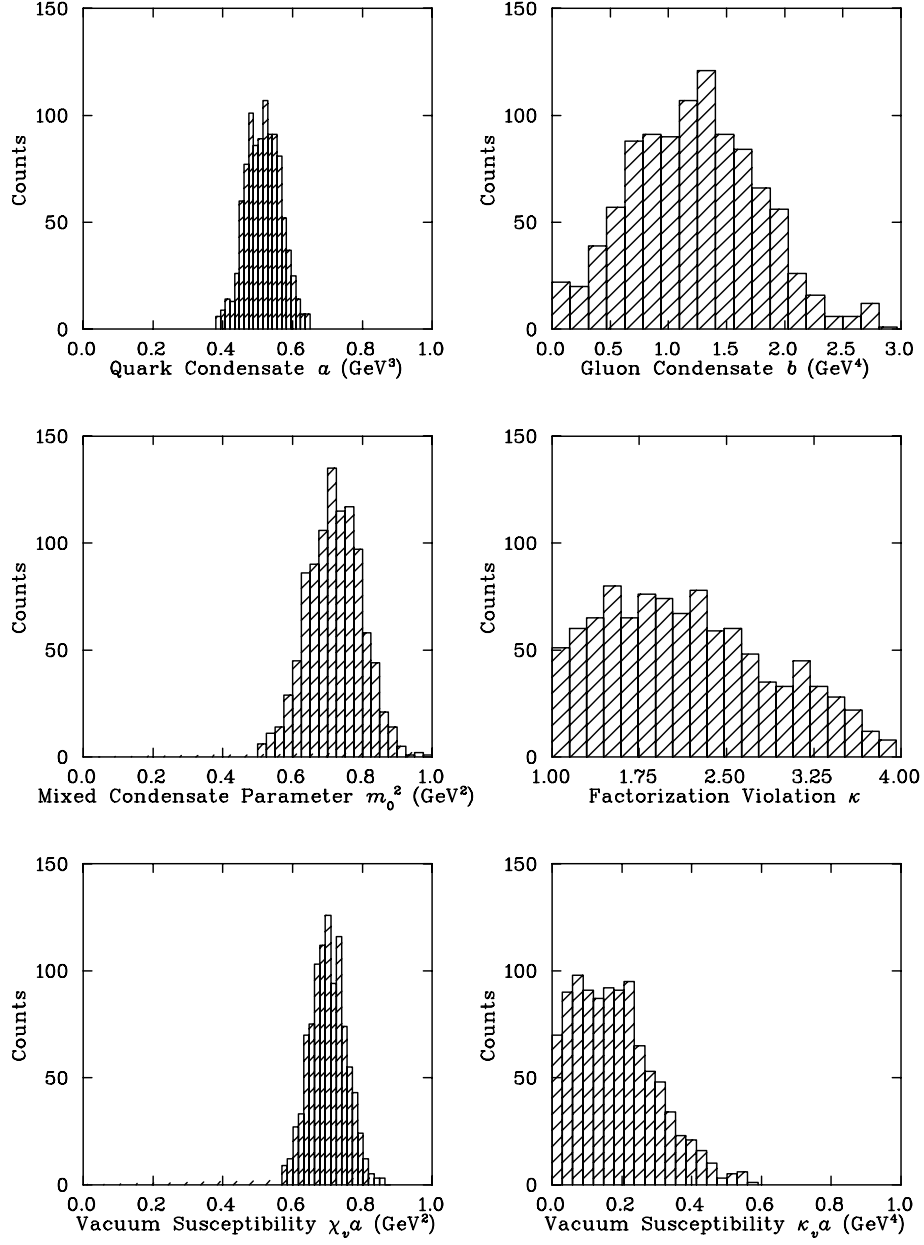


FIG. 1. Distributions for the QCD parameters drawn from a sample of 1000 sets. The vacuum susceptibilities for g_A are shown here.

When performing a Monte-Carlo analysis of a g_A sum rule, we first fit the corresponding mass sum rule(s) to obtain the nucleon mass M_N , pole residue $\tilde{\lambda}^2$ and the continuum threshold w_N . Then, the mass and the pole residue are used in the g_A sum rule where the three remaining parameters including the transition strength A , the continuum threshold w , and g_A are optimized. We impose a physical constraint on w requiring that $w > M_N$, and discard QCD parameter sets that do not satisfy this criteria. The above procedure is repeated for each QCD parameter set until a certain number of sets (typically 1000 sets) are finished.

In doing a full search for the g_A sum rules, we encountered three scenarios regarding the continuum threshold w . First, w falls consistently below the nucleon mass, signaling a failure of the sum rule to resolve the pole from the continuum. In order to proceed in this case, the continuum threshold of the mass sum rule is used in the corresponding g_A sum rule. Note that this is the assumption made in previous works analyzing g_A . Second, we are able to get $w > M_N$ from the search, but the uncertainty on w is uncharacteristically large, a sign of an unstable fit. The origin of the large uncertainty is that the search algorithm occasionally returns very large values for w . Since in the continuum model, the contributions from large w are exponentially damped out, the extracted results for g_A and the transition are not seriously affected. We consider such fits marginally acceptable. One could in principle impose a cutoff on large w in the search algorithm to reduce the uncertainty. We choose not to do so, but rather use it as a performance indicator of the sum rule. Third, we get both $w > M_N$ and reasonable uncertainty. This is the best scenario.

C. Results and Discussion

Now we are ready to examine the sum rules. We find that sum rule (21) at the chirally-odd structure $Z \cdot p \hat{p} \gamma_5$, which has been chosen in previous works, fails to have a valid Borel window. Fig. 2 shows the highest-dimension-operator (HDO) contributions of the QCD side relative to the sum of terms and the continuum-plus-transition contributions relative to the total phenomenological side as a function of the Borel mass. The former is decreasing with the Borel mass while the latter is increasing. Also shown are the HDO contributions at $\beta = 0$, which should be used to determine the lower limit of the Borel window when the 10% criteria is applied [15]. The figure reveals that around a Borel mass of 1 GeV, the HDO contributions are large at about 70%, indicating poor OPE convergence. Only when the Borel mass reaches about 1.8 GeV, do their contributions drop to below 10%. On the other hand, at such Borel mass the continuum contributions increase to about 80%, and almost completely dominate the phenomenology. These continuum model contributions are subtracted from the leading terms of the OPE such that the terms independent of the Borel mass dominate the OPE. This effect trivially explains why in Ref. [10] a plateau was reached when the Borel mass was greater than 1.8 GeV. As a result, any ground state properties extracted from this sum rule are seriously contaminated by short-comings of the excited state model. We analyzed this sum rule using the Monte-Carlo method with 1000 sets of QCD parameters, and the conventional conditions: in the Borel region of 0.9 GeV to 1.2 GeV, with the Ioffe current ($\beta = -1$), and the previous assumption that the continuum threshold in the g_A sum rule is the same as that of the mass sum rule. The result is

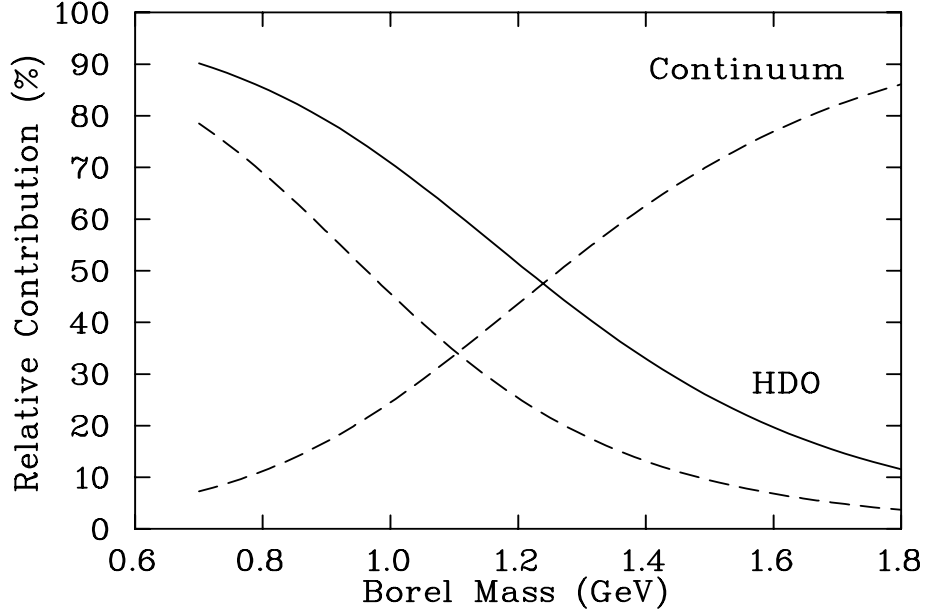


FIG. 2. The HDO contributions of the OPE relative to the sum of terms and the continuum-plus-transition contributions relative to the total phenomenological side are displayed as a function of the Borel mass for sum rule (21) at $\beta = -1.2$ (dashed). The solid line shows the HDO contributions at $\beta = 0$.

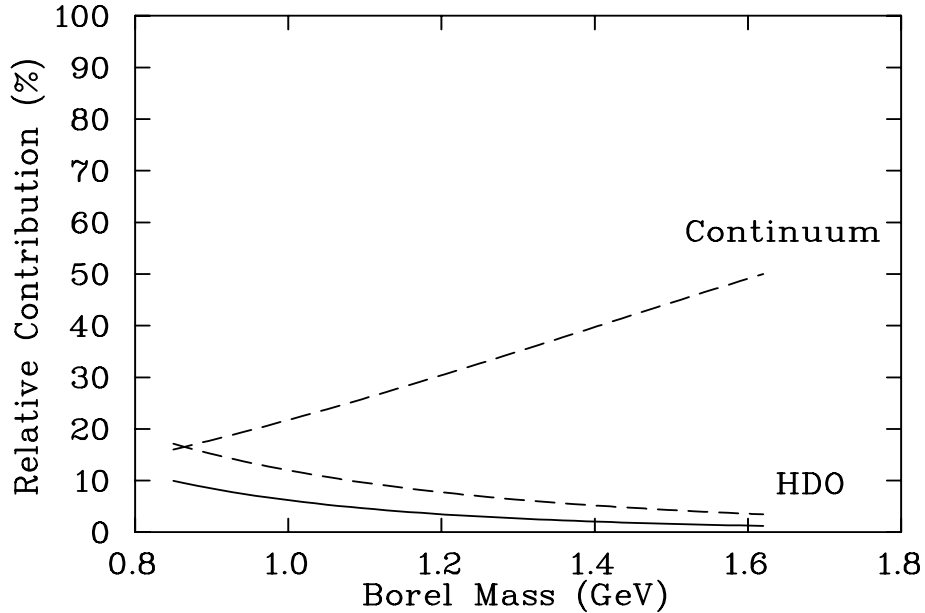


FIG. 3. The valid Borel window for sum rule (21) at optimal $\beta = -1.2$. Both the relative HDO contributions limited to 10% of the OPE and the continuum-plus-transition contributions limited to 50% of the phenomenology are illustrated by dashed lines. Note that the lower limit is determined at $\beta = 0$.

$g_A = 11.0 \pm 4.86$, as compared to 1.26. This example shows the importance of maintaining both OPE convergence and ground state dominance in extracting hadron properties from QCD sum rules.

Having demonstrated the failure of sum rule (21), we now turn to sum rule (22) at the chirally-even structure $iZ_\mu\sigma^{\mu\nu}p_\nu\gamma_5$. This sum rule does have a valid Borel window, as shown in Fig. 3. Within a wide region of about 1 GeV, the HDO contributions to the OPE are less than 10%, and the continuum contributions are less than 50%. Analysis of this sum rule yields $g_A = 1.87 \pm 0.92$, as explained below.

In illustrating how well a sum rule works, we first cast the sum rule into the subtracted form $\Pi_S = c g_A \lambda^2 e^{-M_N^2/M^2}$ where Π_S represents the OPE minus excited state contributions. Here c is a constant factor: 1 for (21), (35), (37), (38); M_N for (20), (22), (32), (33), (34), (36); and $1/M_N$ for (39). Then the logarithm of both sides is plotted against the inverse of M^2 . The right-hand side will appear as a straight line. The linearity of the left-hand side gives a good indication of OPE convergence and the quality of the continuum model. The two curves should match for a good sum rule. This way of matching the sum rules is similar to looking for a ‘plateau’ as a function of Borel mass in the conventional analysis, but has the advantage of not restricting the analysis regime in Borel space to the valid regimes common to *both* two-point and three-point correlation functions.

Fig. 4 shows the fit of (22) in conjunction with (40) at the optimal $\beta = -1.2$. Fig. 5 shows the fits of (33) and (36) in conjunction with (42) and (43) at the optimal $\beta = 0$. For comparison purposes, the corresponding nucleon mass sum rule is also plotted.

Sum rule (22) does not have enough information in the OPE to completely determine the fit parameters, so we have assumed the equivalence of continuum thresholds in two- and three-point functions; $w = w_N$. For curiosity, we also tried to fix the nucleon mass at its known value and found the fits and uncertainties are essentially the same. There are some small deviations from linearity (dashed lines) for the spin-1/2 correlator g_A sum rules, but near perfect linearity for the mixed correlator g_A sum rules. Unfortunately, the error bars for the g_A sum rules are much larger than those of the corresponding nucleon mass sum rules.

Since all the fit parameters in the Monte-Carlo analysis are correlated, one can study the correlations between any two parameters by looking at their scatter plots. Fig. 6 shows the correlations of the QCD input parameters with g_A for sum rule (22). The plots for the quark condensate a , the mixed condensate m_0^2 and the vacuum susceptibility $\chi_v a$ look fairly random, suggesting little correlation. The gluon condensate and the factorization violation parameter display some weak positive correlations with g_A , while the vacuum susceptibility $\kappa_v a$ reveals weak negative correlations. In fact, we found the same correlation patterns between g_A , κ and κ_v in all the sum rules. Fig. 7 shows the correlations of the phenomenological fit parameters with g_A for sum rule (22).

One should bear in mind, however, that the correlations are in general different from sum rule to sum rule. Fig. 8 shows the correlations of the QCD input parameters with g_A for sum rule (36). Fig. 9 shows the correlations of the phenomenological fit parameters with g_A for sum rule (36). There are some subtle differences between the correlations in this sum rule and those in (22). First, g_A is predicted to be positive here in the entire parameter space, unlike (22). Second, the distributions in Fig. 6 are rounded-shaped, while they are more concentrated toward smaller g_A in Fig. 8. Third, the correlations with the gluon condensate

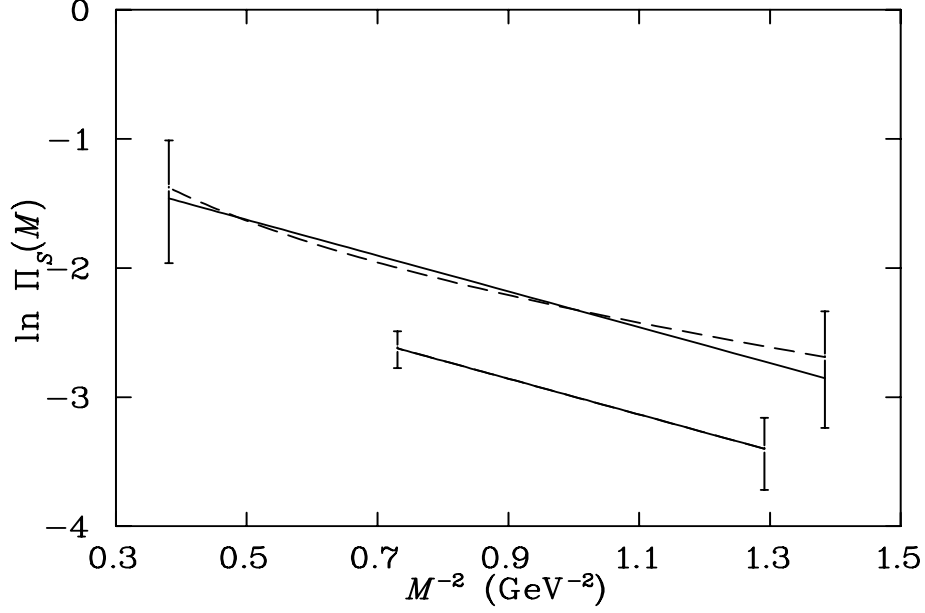


FIG. 4. A six-parameter ($M_N, \tilde{\lambda}_{1/2}, w_N, w, A, g_A$) fit of sum rule (22) in conjunction with (40). The solid line is the ground state contribution: The dashed line (hidden for (40)) is the rest of the contributions (OPE-continuum-transitions). The error bars are only shown at the two ends for clarity.

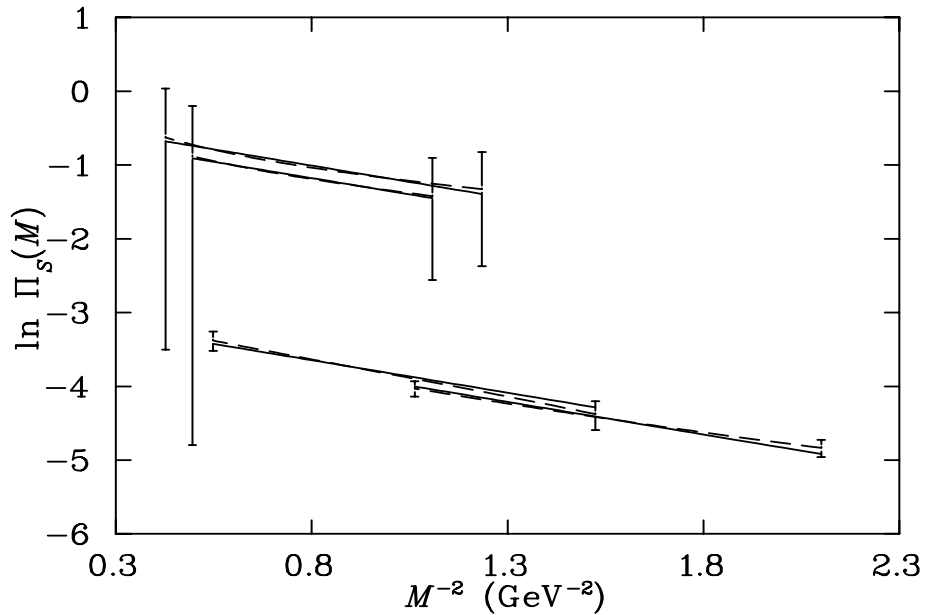


FIG. 5. Same as Fig. 4, except for the mixed correlator sum rules. From top down, the fits are for sum rules (33), (36), (43), and (42). For clarity, the mass sum rule fits are shifted downward by 2 units.

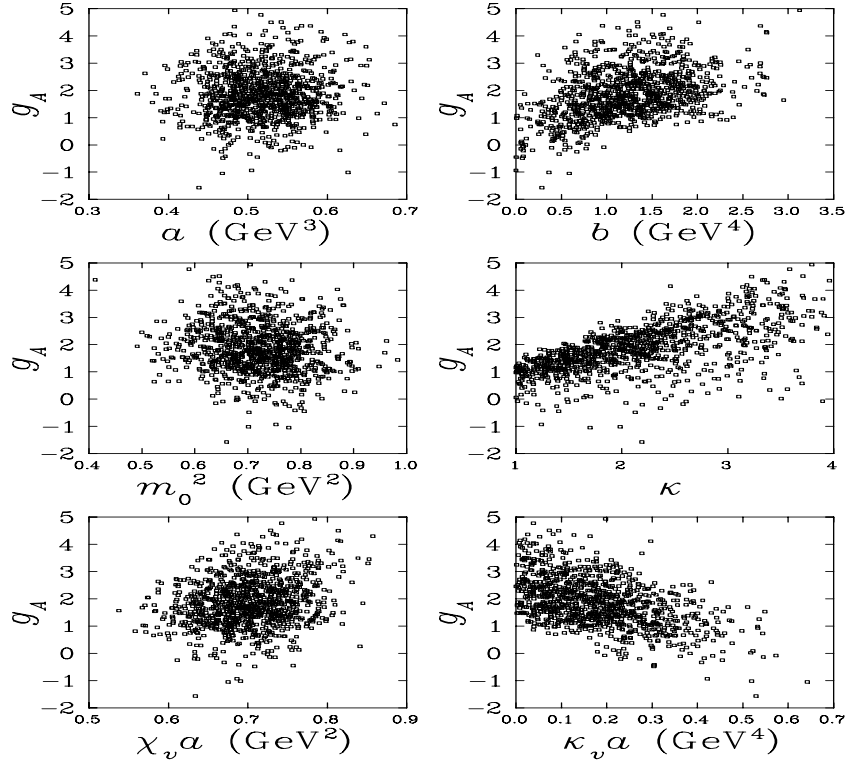


FIG. 6. Scatter plots showing correlations between g_A and the QCD input parameters for sum rule (22).

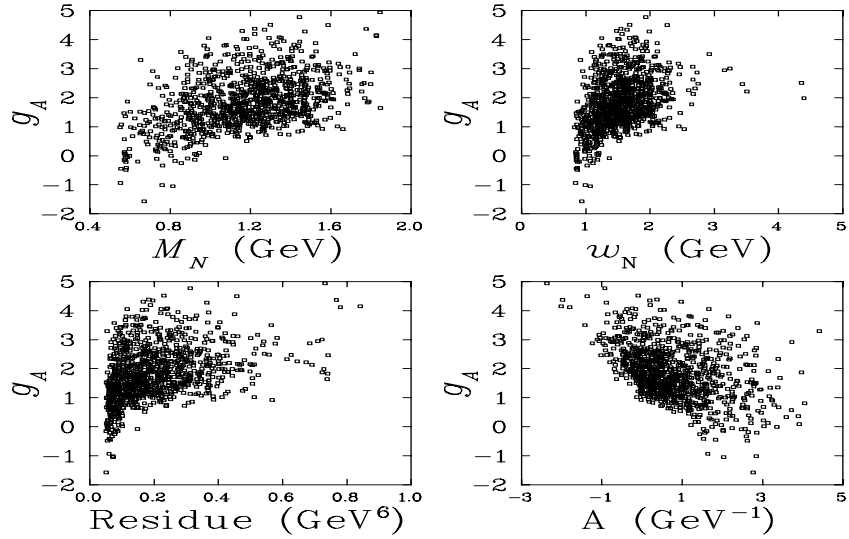


FIG. 7. Scatter plots showing correlations between g_A and the phenomenological fit parameters for sum rule (22).

in (36) are weakly negative, opposite to those in (22). Fourth, the correlations among fit parameters are quite different in the two sum rules. It is interesting to see that in Fig. 9, small values of the pole residue are responsible for large values of g_A and *vice versa*.

We have examined the scatter plots for other sum rules as well. We find that the above differences between the mixed correlator and the spin-1/2 correlator are qualitatively true for other sum rules. It is interesting to observe how different sum rules resolve the same observables in different ways. This reinforces the danger of linking a particular term in the OPE as responsible for a particular observable.

In Table I we give a summary of the results from the consideration of 1000 sets of QCD parameters. Only those sum rules that have valid Borel windows are listed. The presence of a second row indicates that the continuum threshold was successfully searched as an independent parameter (the second or third scenario discussed earlier). Note that sum rule (36) for g_A^8 , g_A^s and g_A^0 has the continuum model term proportional to β . Therefore $\beta = -0.1$ was used instead of $\beta = 0$ in order to maintain a model for excited state contributions in place of additional poles, and enhance the magnitude of the HDO of this sum rule.

The positive statement one can make is that for each coupling, the results are consistent with each other within one standard deviation. The results also agree with the experimental values within one and half standard deviations, although the central values appear to lie consistently above the experimental values. Sum rule (33) consistently predicts larger values for the couplings than the rest. Also the correct ordering $g_A^8 > g_A^s > g_A^0$ is apparent. Unfortunately, the uncertainties in the coupling constants are large at about 50% to 100%, as compared to the nucleon mass obtained from the same method, which only has 10% to 25% errors [see Eq.(41) and Eq.(44)]. The large uncertainties suggest that fine adjustments of the QCD input parameters will allow one to make the central values of the fit parameters reproduce the experimental numbers. At the present stage, we feel that such refinements are not meaningful until the sum rules themselves are derived to a similar accuracy.

When the continuum threshold is included as a search parameter, the only stable results for g_A are from sum rule (36). This sum rule proves to be the best sum rule we derived. The overall effects of searching the continuum threshold appear to cause small increases in the couplings, and small decreases in the transition strengths. However, the uncertainties are too large to allow a definite conclusion. We have compared the quality of the fits with or without searching the continuum threshold and found they are essentially the same.

The origin of the large errors lies mainly in the poorly determined normalization of the two-point function as indicated by the large uncertainty in $\tilde{\lambda}^2$. While we can consider ratios of two- and three-point functions to eliminate the parameter $\tilde{\lambda}^2$, the poorly determined normalization of the two-point function remains. The hope was that the two- and three-point functions would be sufficiently correlated that the poorly determined normalization of the two-point function would mirror that of the three-point function and allow an extraction of g_A with small uncertainties. However, our analysis indicates this is not the case.

Some interplay between g_A and $\tilde{\lambda}^2$ is illustrated in Figs. 7 and in particular 9. The correlations exist because the valid Borel regimes for the sum rules are not identical, and the residue does not factor out as it would in a ratio of sum rules. Fig. 9 displays the tendency for g_A to be small when $\tilde{\lambda}^2$ is large and *vice versa*, as one might expect from the form $g_A \tilde{\lambda}^2 e^{-M_N^2/M^2}$ for the three-point function ground state contribution. We expect the result to be general to any QCD sum rule of nucleon current matrix elements (three-point

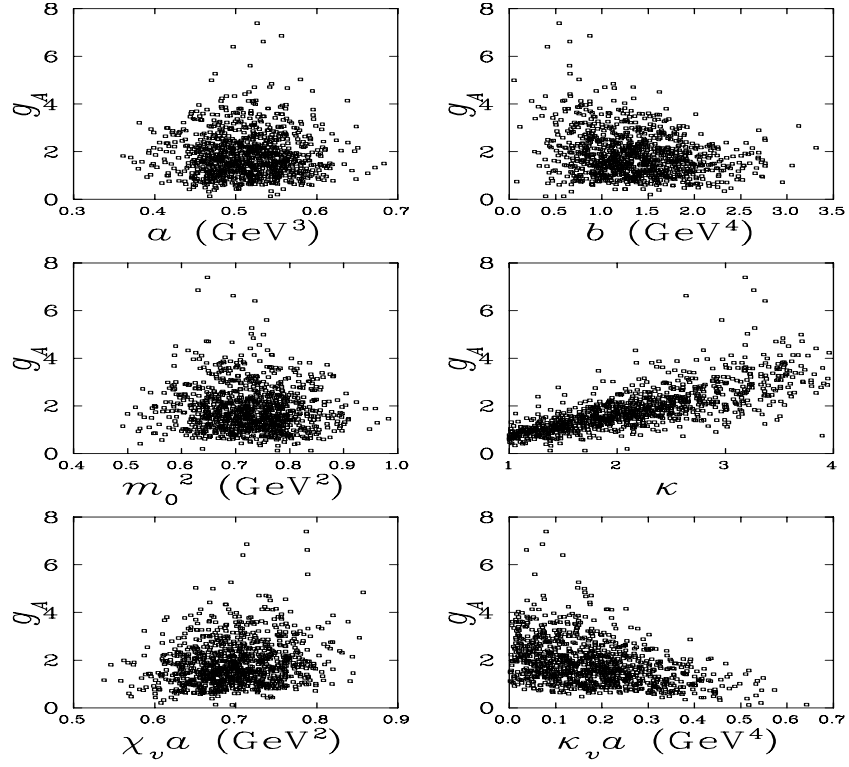


FIG. 8. Scatter plots showing correlations between g_A and the QCD input parameters for sum rule (36).

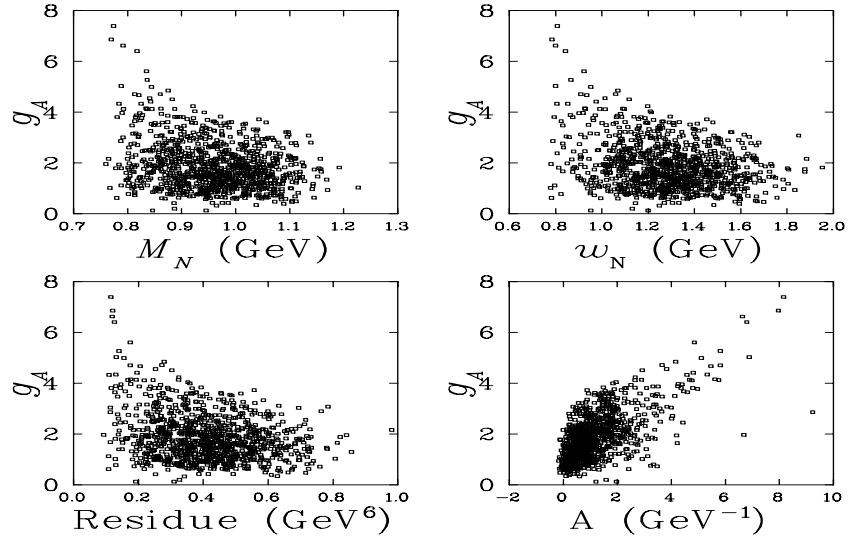


FIG. 9. Scatter plots showing correlations between g_A and the phenomenological fit parameters for sum rule (36).

TABLE I. Monte-Carlo analysis results from consideration of 1000 QCD parameter sets. A second row indicates that the continuum threshold could be searched as an independent parameter for that sum rule. Otherwise, it is assumed to be the same as that of the nucleon mass sum rule. The last column shows the relative contributions of the continuum (including transitions) to the phenomenological side in the given Borel window.

Sum Rule	Borel Window (GeV)	g_A	A (GeV ⁻¹)	w (GeV)	Continuum
(22)	0.85 to 1.62	1.87± 0.92	0.77± 0.97		29% to 50%
(33)	0.90 to 1.53	2.52± 1.31	0.40± 0.95		20% to 50%
	0.90 to 1.55	3.53± 1.44	-0.72± 0.43	3.49±4.73	20% to 50%
(36)	0.95 to 1.42	1.88± 0.94	1.20± 1.13		31% to 50%
	0.95 to 2.34	2.38± 1.07	0.96± 0.92	2.08±0.42	20% to 50%
Sum Rule	Borel Window (GeV)	g_A^8	A (GeV ⁻¹)	w (GeV)	Continuum
(22)	0.67 to 1.16	2.26± 2.28	-1.49± 2.42		22% to 50%
(33)	0.71 to 1.60	2.55± 1.10	0.13± 0.86		0.6% to 50%
(36)	1.10 to 1.23	1.43± 0.84	1.28± 1.06		46% to 50%
	1.10 to 1.50	1.57± 0.82	1.03± 0.80	2.97±9.25	36% to 50%
Sum Rule	Borel Window (GeV)	g_A^s	A (GeV ⁻¹)	w (GeV)	Continuum
(33)	0.59 to 1.04	1.97± 1.43	-1.33± 0.72		21% to 50%
(36)	0.96 to 1.95	0.70± 0.58	0.51± 0.63		33% to 50%
	0.96 to 1.96	1.06± 0.51	0.51± 0.41	3.72±5.40	11% to 50%
(39)	0.73 to 1.01	0.67± 0.47	0.94± 0.76		34% to 50%
Sum Rule	Borel Window (GeV)	g_A^0	A (GeV ⁻¹)	w (GeV)	Continuum
(33)	0.64 to 0.70	0.81± 0.99	-1.36± 1.20		45% to 50%
(36)	0.77 to 1.70	0.39± 0.30	-0.12± 0.22		12% to 50%
	0.77 to 1.74	0.55± 0.28	-0.02± 0.10	3.66± 3.15	12% to 50%

functions) from the linear response of the external-field. Only when the external-field is treated non-perturbatively, might the drawback be avoided [14].

Other sources of uncertainty are in the poorly known vacuum susceptibility κ_v and in the factorization approximation of higher order operators. From correlation studies we discovered that the sum rules seem to favor smaller factorization violation and larger vacuum susceptibility κ_v . Better estimates of these parameters are clearly needed.

The presence of the transitions is an additional source of contamination not found in two-point functions. To see the role the transitions play, it is useful to cast the sum rule in the form $g_A + AM^2 = \dots$. By matching the two sides over some region in M^2 where a linear behavior is observed, one can extract g_A from the intercept of the straight line with the y-axis. In fact this is the method explicitly used in previous analyses to extract g_A , except that some combinations with the mass sum rule or other sum rules were used. It is clear that the transitions play a crucial role since they determine the slope of the line from which g_A is extracted. Small changes in the transition strength A can lead to quite different values of g_A .

VI. ALTERNATIVE TREATMENT OF THE TRANSITIONS

As discussed in Sec. IV A, the transitions between the ground state and the excited states lead to off-diagonal contributions that are not exponentially suppressed relative to the ground state. We have seen in the previous section that these off-diagonal contributions play important roles since they determine the curvature from which g_A is extracted. As can be seen from Eq. (29), the contribution from the transitions is in general a complicated function of the Borel mass. The usual treatment of crudely modeling the transitions by a constant parameter (multiplied by $e^{-M_N^2/M^2}$) could have significant impact on the determination of g_A . Recently, a new formalism for treating the transitions has been pointed out in Ref. [22]. In this new formalism, the transition contribution is exponentially suppressed relative to the ground state contribution and hence can be included in the continuum model. Here we briefly illustrate the new formalism. The reader is referred to Ref. [22] for further details and discussions.

Let us consider the phenomenological representation of Eq. (28). If one first multiplies the expression with the factor $(p^2 - M_N^2)$, then performs the Borel transform, one sees that the transition contributions are exponentially suppressed relative to the ground state contributions. As a result, one can use the conventional pole plus continuum model on the phenomenological side. The physics behind such a manipulation is a rearrangement of information: the transition strength on the phenomenological side is not lost, but gets absorbed into the new continuum model built from an altered OPE. So it is important in this new formalism to treat the continuum threshold as an independent phenomenological parameter to be extracted from the sum rule along with the ground state property of interest. This point has been emphasized in Ref. [22], where an example was given in the scalar channel. (This point, however, was completely ignored in Refs. [23–25], where a similar formalism was adopted).

The sum rules in this new formalism can be obtained from the standard ones by the following substitutions. On the OPE side, $M^6 \rightarrow 3M^8 - M_N^2 M^6$, $M^4 \rightarrow 2M^6 - M_N^2 M^4$, $M^2 \rightarrow M^4 - M_N^2 M^2$, $M^0 \rightarrow -M_N^2$, $1/M^2 \rightarrow -(1 + M_N^2/M^2)$, $1/M^4 \rightarrow -(1/M^2 + M_N^2/2M^4)$. The E factors associated with powers of the Borel mass are suppressed for clarity. On the phenomenological side, for the spin-1/2 correlator, one replaces the right hand side of Eq. (20) to Eq. (22) by $c \tilde{\lambda}_{1/2}^2 g_A e^{-M_N^2/M^2}$, where c is $2M_N^2$, -1 , $-M_N$, respectively. Similarly the phenomenological side of the mixed correlator becomes $c \tilde{\lambda}_{1/2} \tilde{\lambda}_{3/2} g_A e^{-M_N^2/M^2}$, where c is $2M_N^2$, $2M_N$, $-M_N$, -1 , $-M_N$, -1 , -1 , $-1/M_N$, for Eq. (32) to Eq. (39), respectively. We will denote these modified sum rules by appending a symbol (PC) indicating pole+continuum phenomenology to their standard counterparts.

In Table II we summarize all the results from a Monte-Carlo analysis of 1000 QCD parameter sets using the new formalism. For comparison purposes, we also list the results from not searching the continuum threshold.

The results for the coupling constants are qualitatively the same as those in the standard approach. This suggests that the main source of error in g_A is not in the treatment of transitions. However, the new formalism does show the potential for improvement. For example, the Borel windows become generally wider, the continuum contributions become smaller, and the numerical fits are generally more stable. Future studies should take advantage of

TABLE II. Same as Table I, except they are obtained from the new pole-plus-continuum sum rules, as indicated by (PC).

Sum Rule	Borel Window (GeV)	g_A	w (GeV)	Continuum
(22)(PC)	0.82 to 1.83	1.44 ± 0.59		2.3% to 50%
(33)(PC)	0.84 to 1.40	2.80 ± 1.50		9% to 50%
(36)(PC)	0.84 to 1.65	3.60 ± 1.76	2.22 ± 0.62	0.5% to 50%
	0.95 to 1.60	2.02 ± 1.02		9.3% to 50%
(36)(PC)	0.95 to 1.81	2.44 ± 1.12	2.15 ± 0.48	10% to 50%
Sum Rule	Borel Window (GeV)	g_A^8	w (GeV)	Continuum
(22)(PC)	0.65 to 1.36	1.40 ± 1.03		2% to 50%
(33)(PC)	0.65 to 1.65	1.75 ± 1.22	2.48 ± 2.08	0% to 50%
	0.67 to 1.48	2.44 ± 1.30		2% to 50%
(36)(PC)	0.67 to 1.77	3.19 ± 1.54	2.39 ± 0.57	0% to 50%
	1.13 to 1.96	1.43 ± 0.75		9% to 50%
(36)(PC)	1.13 to 2.17	1.65 ± 0.84	2.07 ± 0.78	9% to 50%
Sum Rule	Borel Window (GeV)	g_A^s	w (GeV)	Continuum
(22)(PC)	0.52 to 1.09	0.62 ± 1.48		1% to 50%
(33)(PC)	0.52 to 1.33	0.54 ± 0.99	2.16 ± 2.26	0% to 50%
	0.57 to 1.24	1.20 ± 0.94		2% to 50%
(36)(PC)	0.57 to 1.50	1.56 ± 1.08	2.39 ± 2.15	0% to 50%
	0.98 to 1.68	0.79 ± 0.63		9% to 50%
(36)(PC)	0.98 to 1.90	0.97 ± 0.62	2.30 ± 0.97	1% to 50%
Sum Rule	Borel Window (GeV)	g_A^0	w (GeV)	Continuum
(22)(PC)	0.45 to 1.03	-0.36 ± 0.90		0.3% to 50%
(33)(PC)	0.60 to 0.91	0.36 ± 0.59		9% to 50%
(36)(PC)	0.60 to 1.11	0.56 ± 0.59	2.22 ± 1.79	0.5% to 50%
	0.76 to 1.44	0.42 ± 0.32		5% to 50%
(36)(PC)	0.76 to 1.68	0.51 ± 0.36	2.16 ± 1.27	5% to 50%

the new formalism to avoid the errors associated with the approximation in modeling the unwanted transitions.

Although the extracted couplings appear to agree within uncertainties with or without searching the continuum thresholds, there are qualitative differences between the two. To demonstrate this, we show in Fig. 10 the fits for sum rule (22)(PC), (33)(PC) and (36)(PC), without searching the continuum threshold. In Fig. 11 we show the two successful fits obtained when searching the continuum threshold. We see that the two sides of the sum rules do not match very well when the continuum threshold is not searched. The match improves significantly for the mixed correlator sum rules when the continuum threshold is searched. A large uncertainty was found for the searched continuum threshold in sum rule (22)(PC). This suggests that it is really unable to separate the pole from the continuum.

The above results confirm that the continuum threshold in the new formalism is relied upon to compensate for the transition strength that was explicitly taken into account in the standard approach. Fixing it in the new approach would introduce an artificial bias

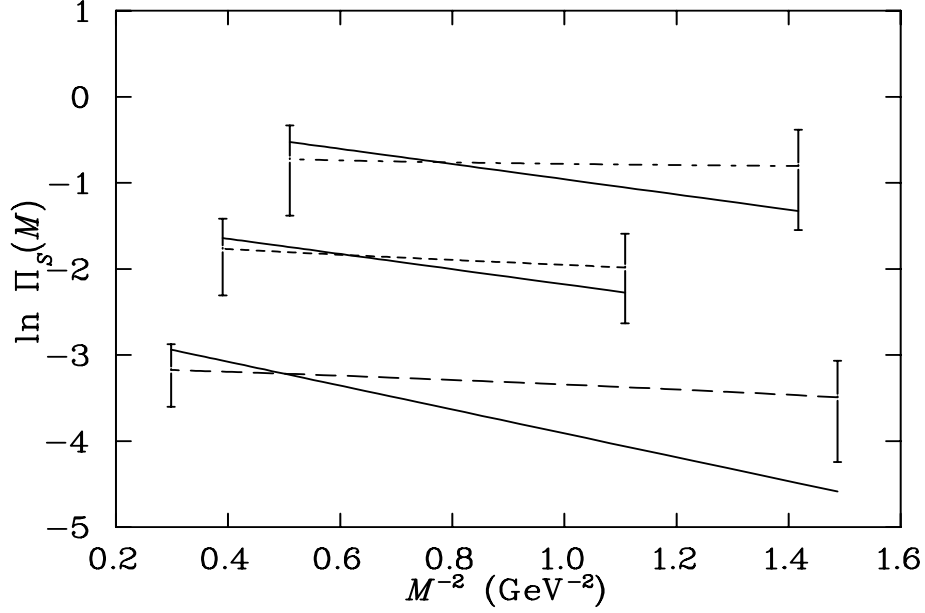


FIG. 10. From top down, Monte-Carlo based fits for g_A from sum rules (33)(PC), (36)(PC), and (22)(PC). The continuum thresholds are assumed the same as that of the corresponding mass sum rules. The solid line is the ground state contribution, and the dashed line is the OPE minus continuum. For clarity, the fits for (36)(PC) and (22)(PC) are shifted downward by 1 unit, respectively.

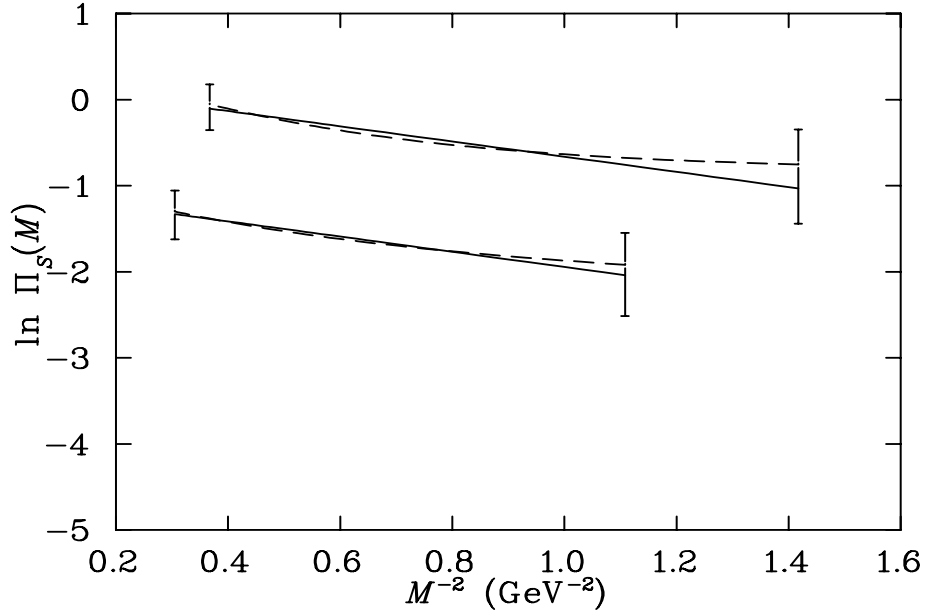


FIG. 11. From top down, fits of sum rules (33)(PC) and (36)(PC) in which the continuum threshold was searched successfully.

to the extracted ground state spectral properties. This is in contrast with the situation in the standard approach. There the OPE was not altered and the transitions were modeled explicitly. As a result, the quality of the fits with or without searching the continuum thresholds was essentially the same.

VII. SUMMARY AND CONCLUSIONS

We have derived eleven new QCD sum rules for the nucleon axial vector coupling constants using the external-field method and generalized interpolating fields. Three are from the spin-1/2 correlator, which can be reduced and compared to those in the literature. Eight are from the mixed correlator, which are new. Using the Monte-Carlo analysis, we are able to determine the predicative ability of the new sum rules for g_A for the first time.

The main advantage of the Monte-Carlo analysis is that it takes into account all uncertainties in the QCD input parameters simultaneously, allowing a quantitative study of how the uncertainties in the QCD input parameters propagate to the phenomenological fit parameters. The method carefully monitors the OPE convergence and the ground-state dominance, the two key criteria in order for the QCD sum rule method to work. Together they determine the Borel window over which the two sides of the sum rules are matched. Those sum rules which do not have a valid Borel window are considered unreliable and therefore discarded. Conventional QCD sum rule analysis is limited to only a small portion of the QCD parameter space, and often the uncertainties assigned to the fit parameters are not based on rigorous error analysis but rather have a certain degree of arbitrariness.

Our most important findings in this work are: a) The nucleon axial vector coupling constants calculated from standard QCD sum rule method have large uncertainties associated with them, approximately 50% to 100%, as compared to the nucleon mass obtained from the same method which has only 10% to 25% error. Within uncertainties, the numbers obtained from different sum rules are consistent with each other and with the experimental values at 1.5σ . The correct ordering in magnitude of the coupling constants, $g_A^s > g_A^s > g_A^0$, is also predicted by the sum rules. b) Sum rule (21), upon which the previous analyses of g_A are based, has poor OPE convergence and poor ground-state dominance properties. The results extracted from this sum rule are unreliable. Both of these findings contradict the conventional wisdom. Traditionally, 10% to 20% errors are often claimed for g_A from QCD sum rule calculations without rigorous error analysis. The selection of sum rule (21) was based upon similarities with the mass sum rule [8] at the structure \hat{p} , which was shown to have poor convergence properties [15], or dimension arguments [7]. Our Monte-Carlo analysis has shown that such criteria may not be reliable in selecting sum rules.

The origin of the large errors in g_A is three-fold. First, it is in the poorly determined nucleon mass sum rules, which are used to normalize the couplings extracted from the form $g_A \tilde{\lambda}^2 e^{-M_N^2/M^2}$. Second, two new parameters are needed to describe the response of the QCD vacuum to the external field. These new parameters introduce additional uncertainties, especially the vacuum susceptibility κ_v which is very poorly known. Third, the transitions between the ground state and the excited states caused by the probing axial current is another source of uncertainty. Their contributions are not exponentially suppressed relative to the ground state and must be included in the spectral representation. Little is known about

these transitions. The standard approach is to introduce a new phenomenological parameter to account for all the contributions from the transitions. Usually the new parameter is assumed to be constant, but in fact it depends in some complicated way on the Borel mass. The approximation may have a sizable impact on the results since it plays a crucial role in the extraction of g_A . In any event, the presence of an additional unknown parameter leads to larger uncertainties in g_A .

To further investigate the role of the transitions, we have studied an alternative treatment which can lead to exponential suppression of their contributions relative to the ground state. As a result, one can apply the traditional pole-plus-continuum model in the phenomenological representation. The contributions of the transitions are not lost, but simply get absorbed in the new continuum model. So it is important in this formalism to search the continuum threshold as an independent parameter. The results for the coupling constants are similar to those in the standard approach. This implies that the main source of error is not in the treatment of transitions, but in the pole residues and the vacuum susceptibilities. However, there are advantages to be gained with the new formalism. The Borel windows become generally wider, and the numerical fits are generally more stable. Future studies should take advantage of the method to avoid errors associated with the approximation of modeling of the unwanted transitions.

As for the question of valid sum rules for g_A , our Monte-Carlo analysis reveals that only three out of the eleven sum rules are able to resolve the ground state properties from the continuum. They are sum rule (22) from the spin-1/2 correlator, (33) and (36) from the mixed correlator. Even the three valid sum rules perform differently. Sum rule (36) has the best performance in terms of allowing a full search and the stability of the results. It is followed by sum rule (33), then by (22). We find that in general the mixed correlator sum rules perform better than the spin-1/2 correlator sum rules, similar to the situation for the nucleon mass sum rules.

Study of correlations among the input and fit parameters reveals how a particular sum rule resolves the ground state from the continuum. We find that g_A does not have strong correlations with the quark condensate, the mixed condensate, the gluon condensate, nor the vacuum susceptibility χ_v . g_A has some weak positive correlations with the factorization violation parameter κ , and some weak negative correlations with the vacuum susceptibility κ_v . These correlations can give some hints on what values for κ and κ_v are preferred by the self-consistency requirement in the sum rules. We should stress that correlation patterns are different for different sum rules. The above observations are some general trends displayed by all the valid sum rules, despite some subtle differences.

As to the problem of how to reduce the large uncertainties in g_A from QCD sum rule calculations, one may attack it from several directions as suggested from the discussion of their origins: a) improved accuracy of the QCD sum rules, b) better estimates of the vacuum susceptibilities, especially κ_v , and c) better treatment of the transitions. Of these, point a) is the most important. One way to improve the accuracy of the sum rules is to reduce the uncertainties in the QCD input parameters. However, there is a limit on it. As shown in Ref. [15], the best one can do with current implementation of the QCD sum rule approach is 25% for the two-point function normalization. Reduction of this uncertainty to the 10% level requires 5% uncertainties on the QCD input parameters. But this level of accuracy is beyond

the current state of the art as indicated by the unacceptably large χ^2/N_{DF} . We believe the future lies in improving the sum rules themselves. Examples may include incorporating α_s corrections, higher order power corrections, and devising alternative interpolating fields that result in better sum rules, as done here.

Finally, we want to point out that although this work is focused on g_A , the conclusions are expected to apply to other nucleon current matrix elements. The presence of large uncertainties in nucleon matrix elements indicate that only small adjustments of the QCD input parameters are required to reproduce the measured values. Likewise, small fluctuations in the input parameters can lead to large fluctuations in the matrix elements, such that most QCD sum rule calculations of matrix elements in the literature are likely to have 50% uncertainties at best, given the current implementation of the QCD sum rule formalism.

ACKNOWLEDGMENTS

This work is supported in part by the Natural Sciences and Engineering Research Council of Canada and U.S. DOE under grants DE-FG03-93DR-40774 (F.L.), DE-FG06-88ER-40427 (D.L.) and DF-FC02-94ER-40818 (X.J.).

REFERENCES

- [1] L. Montanet *et. al.*, Phys. Rev. D **50**, 1173 (1994).
- [2] F.E. Close and R.G. Roberts, Phys. Lett. **B316**, 165 (1993).
- [3] J. Ashman *et. al.* (EMC), Phys. Lett. **B206**, 364 (1988); Nucl. Phys. **B328**, 1 (1989).
- [4] D. Adams *et. al.* (SMC), Phys. Lett. **B329**, 399 (1994).
- [5] K. Abe *et. al.* (E143), Phys. Rev. Lett. **74**, 346 (1995).
- [6] M.A. Shifman, A.I. Vainshtein, and Z.I. Zakharov, Nucl. Phys. **B147**, 385, 448 (1979).
- [7] V.M. Belyaev and Ya.I. Kogan, Phys. Lett. **136B**, 273 (1984).
- [8] C. Chiu, J. Pasupathy, and S. Wilson, Phys. Rev. D **32**, 1786 (1985).
- [9] S. Gupta and M. Murthy, Phys. Rev. D **39**, 2547 (1989).
- [10] E.M. Henley, W.-Y. P. Hwang, and L.S. Kisslinger, Phys. Rev. D **46**, 431 (1992).
- [11] V.M. Belyaev, B.L. Ioffe, and Ya.I. Kogan, Phys. Lett. **151B**, 290 (1985).
- [12] B.L. Ioffe and A. Yu. Khodzhamiryan, Sov. J. Nucl. Phys. **55**(11), 1701 (1992).
- [13] V.A. Novikov, M.A. Shifman, A.I. Vainshtein, M.B. Voloshin and V.I. Zakharov, Nucl. Phys. **B237**, 525 (1984).
- [14] M. Burkardt, D.B. Leinweber, and X. Jin, Phys. Lett. **B385**, 52 (1996).
- [15] D.B. Leinweber, University of Washington Report No. UW-DOE/ER/40427-17-N95, nucl-th/9510051 (1995), accepted for publication in *Annals of Physics*.
- [16] D. B. Leinweber, Phys. Rev. **D51**, 6369, 6383 (1995).
- [17] K.-F. Liu, hep-lat/9510046, and references therein.
- [18] X. Jin and D.B. Leinweber, Phys. Rev. C **52**, 3344 (1995).
- [19] M.J. Iqbal, X. Jin, and D.B. Leinweber, Phys. Lett. **B386**, 55 (1996).
- [20] R.J. Furnstahl, X. Jin, and D.B. Leinweber, Phys. Lett. **B387**, 253 (1996).
- [21] B.L. Ioffe and A.V. Smilga, Nucl. Phys. **B232**, 109 (1984).
- [22] X. Jin, TRIUMF Report No. TRI-PP-96-13, hep-ph/9608303 (1996), to appear in Phys. Rev. D **55**, (1997).
- [23] I. I. Balitsky and A. V. Yung, Phys. Lett. **129B**, 328 (1983).
- [24] V. M. Braun and A. V. Kolesnichenko, Nucl. Phys. **B283**, 723 (1987).
- [25] H. He and X. Ji, Phys. Rev. D **52**, 2960 (1995); hep-ph/9607108 (1996).